

Article

# A Closed-loop Approach to Fight Coronavirus: Early Detection and Subsequent Treatment

Guoguang Rong<sup>a,b,c</sup>, Yuqiao Zheng<sup>a,b,c</sup>, Xi Yang<sup>a,b,c</sup>, Kangjian Bao<sup>b,c</sup>, Fen Xia<sup>a,b,c</sup>, Huihui Ren<sup>b,c</sup>, Sumin Bian<sup>a,b,c</sup>, Lan Li<sup>b,c</sup>, Bowen Zhu<sup>b,c</sup> and Mohamad Sawan<sup>a,b,c,\*</sup>

<sup>a</sup>CenBRAIN Neurotech, School of Engineering, Westlake University, Hangzhou 310024, China

<sup>b</sup>School of Engineering, Westlake University, Hangzhou 310024, China

<sup>c</sup>Institute of Advanced Study, Westlake Institute for Advanced Study, Hangzhou 310024, China

\*Corresponding author: sawan@westlake.edu.cn

**ABSTRACT** - The recent COVID-19 pandemic has caused tremendous damage to social economy and people's health. Some major issues fighting COVID-19 include early and accurate diagnosis and the shortage of ventilator machines for critical patients. In this work, we propose a closed-loop solution to deal with COVID-19: portable biosensing and wearable photoacoustic imaging for early and accurate diagnosis of infection and magnetically neuromodulation or minimally invasive electrical stimulation to replace the traditional ventilation. Proposed technique can guarantee ubiquitous and onsite detection, and electrical hypoglossal stimulator can be more effective in helping severe patients as well as reducing complications caused by ventilators.

**Keywords:** Biosensing; Coronavirus; SARS-CoV-2; COVID-19; Early diagnosis; Epidemic control; Respiration monitor; Photoacoustic imaging; Neurostimulation

## 1. Introduction

Since December 2019, there has been a large outbreak of COVID-19 pneumonia worldwide, which has caused a great impact on economic development and social operation. This new coronavirus pneumonia is caused by infection of SARS-CoV-2 virus and is an acute respiratory infection. An important reason for the outbreak of COVID-19's epidemic is that the current detection methods are slow and inefficient. In the process of detection and treatment, large and medium-sized medical devices and equipment are involved. Large number of patients are likely to cause the collapse of existing medical system. The main medical instruments used in the existing COVID-19 detection and treatment stage, including Polymerase Chain Reaction (PCR) test, Computed Tomography (CT) scanning instrument and ventilator, require long evaluation time, most corresponding equipment are bulky and expensive, and requires professional operation of these equipment, making it difficult to be applied on a large scale. Therefore, portable, and easy-to-operate detection platform with automatic data-processing system running algorithm is proposed to increase the detection and treatment efficiency.

At present, the detection of COVID-19 needs to be completed by medical authorities in clinical conditions with the prevention of the Center for Disease Control. The main technology is based on polymerase chain reaction, a kind of nucleic acid amplification test (NAAT) [1]. However, nucleic acid extraction and amplification is a complex process. The accuracy of the results is affected by the experiences of operators, the cleanliness of the environment and the timeliness of sample delivery. Therefore, although NAAT method, represented by PCR, has high sensitivity and specificity, the successful detection rate is still low, the result turn-around time is long (typically >4 hours), and frequency and population coverage are limited [2]. Although some agencies have proposed COVID-

19 on-site detection solutions, such as isothermal NAAT, automatic nucleic acid extraction NAAT, and on-site NAAT in mobile laboratory, these methods only try to minimize human factors in nucleic acid extraction and amplification or create a relatively clean environment at the detection site to improve reliability. In fact, they still face the problems of long detection cycle and sample pollution caused by sample transmission and cannot achieve rapid detection and fast delivery of results.

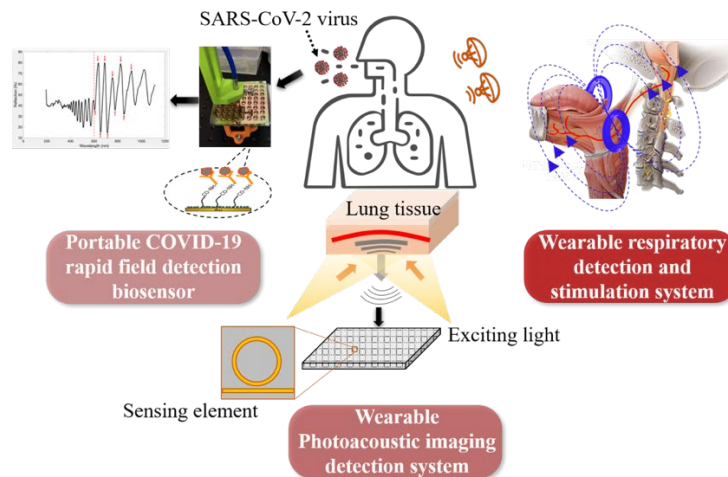


**Fig. 1.** Proposed closed-loop solution for COVID-19, including three main parts: portable biosensor, wearable photoacoustic imaging, and breath detection and magnetic as well as electrical stimulation.

These factors limit the application of NAAT detection in the prevention and control of COVID-19. To detect COVID-19 infected people more accurately, CT scan was used to make lung imaging in the clinic setting. The lung injury was detected and combined with the results of clinical PCR and antibody tests to comprehensively diagnose the infection. However, CT can only be completed in hospitals, Center for Disease Control (CDC) and other institutions, which is difficult to popularize on a large scale. Moreover, CT scan necessitates a long processing time, the subjects need to queue up in turn, and cross infection is easy to occur in the process of queuing. In addition, in the early stage of infection, the pathological characteristics of lung tissue are not obvious enough, as such, its role in early population screening is limited [3]. After infection by SARS-CoV-2, patients are prone to symptoms of dyspnea, especially for critical patients. They need ventilator to help them breathe. However, once patients begin to use the ventilator, they cannot easily leave the ventilator and breathe independently, and some patients may have complications [4].

In view of these realities and the needs for epidemic prevention and control, it is urgent to achieve rapid, low-cost, on-site detection of COVID-19, especially an efficient way to quickly screen infected persons in a large population. Such technical means can help epidemic prevention personnel quickly implement the corresponding isolation, diagnosis, treatment, and recovery processes, and provide a solid technical foundation for epidemic prevention and control and resumption of social activities. In view of this, we propose an efficient COVID-19 solution scheme covering the whole process of early, middle, and late stages of disease development, including the technical means of *in vitro* diagnostic technology, tissue imaging detection technology, breath detection and electrical stimulation technology. With such large span and wide coverage, we aim to innovate for all aspects of COVID-19's influence on human body as far as possible. Moreover, the technical means adopted in this work are based on the rapid application on site, such as portable or wearable devices. The goal is to facilitate the deployment on complex sites and get rid of the dependence on large instruments and a professional environment.

As shown in Figure 1, the three main parts of this project include: 1) A portable COVID-19 rapid field detection biosensor, which can detect trace virus particles from swab, sputum, saliva and bronchoalveolar lavage fluid, and directly detect virus infection from biochemical, microbiological and *in vitro* diagnostic level. Meanwhile, compared to rapid antigen test, the biosensing system has higher sensitivity and lower limit of detection (around 100 copies/ml vs. 10,000 copies/ml), better specificity, lower cost (<1 \$ per test), and higher throughput (>384 tests per half hour); 2) A wearable nanoimaging detection system based on photoacoustic imaging method to scan the upper respiratory tract or lung tissue, in order to detect the change of blood oxygen content in the tissues or blood vessels invaded by the virus before the onset of symptom. This technology can capture the subtle signs of virus infection from the tissue imaging level; and 3) A novel respiration detection and stimulation system, which first detects respiratory abnormalities caused by COVID-19 infection, then applies electrical/magnetic stimulation to assist breathing difficulties or to restore spontaneous breathing to patients who rely on a ventilator. This can detect COVID-19 infection and relieve clinical symptoms.

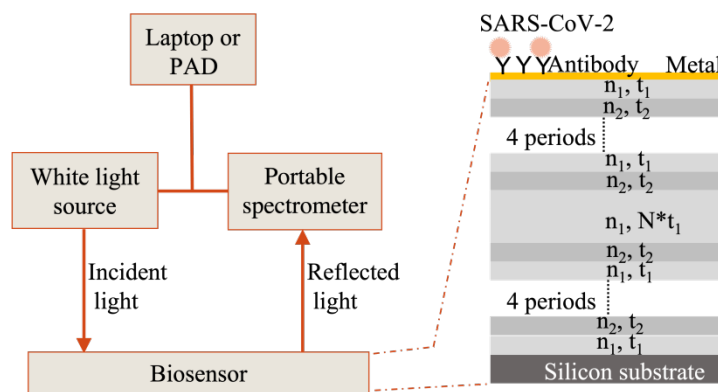


**Fig. 2.** Biosensor and its portable detection system. Two different porous silicon layers construct the resonant microcavity, with optical refractive index and thickness of  $n_1, t_1$  and  $n_2, t_2$ . There are two 4-periods structures sandwiching a defect layer with thickness  $N$  times  $t_1$ .  $N$  can be any number except 1. For details, see reference [5]. Due to nanoporous structures of porous silicon, conformally deposited metal thin film is also nanoporous, which allows LSPR excitation by incident light.

The above three main directions of this work can complement COVID-19's early infection, medium-term development, and the whole process of intensive care. The effective combination of these directions will provide powerful tools for epidemic prevention, control and treatment, and the applications will produce significant social and economic benefits. For example, the combination of portable *in vitro* diagnosis and wearable photoacoustic imaging can quickly diagnose infected people at an early stage and can be applied to population screening because of its high efficiency and speed. For another example, the combination of wearable photoacoustic imaging and respiratory detection and stimulation system can be applied in moderate and severe patients, accurately grasping the patient's condition development in combination with tissue injury and clinical respiratory status and applying electrical stimulation to relieve symptoms before using ventilator and intubation oxygen delivery, to provide valuable time for clinical treatment.

## 2. Proposed system modules

### 2.1. Portable biosensing

Figure 2 shows the schematic diagram of the biosensor and its portable detection system. This sensing device is based on a combination of porous silicon resonant microcavity with localized surface plasmon resonance (LSPR). Porous silicon microcavity includes top and bottom distributed Bragg reflector (DBR), and a defect layer has resonant feature of high-quality factor in its reflection spectrum [5]. The thin metal film conformally deposited on porous silicon also has nanoporous structures, which allows excitation of LSPR resonant mode by incident light. LSPR has strong electromagnetic field confinement in the vicinity of the nanoporous metal thin film. The mode coupling between resonant microcavity and LSPR provides high sensitivity towards virus binding on biosensor surface [6]. The high-quality resonant feature of the resonant microcavity makes it optimal to resolve small shift caused by low virus concentration in specimen.

The detection of the biosensor is based on reflection spectroscopy. Portable and low-cost fiber spectrometer can be used to obtain the reflection spectrum of the biosensor. The biosensor surface has been coated by a specific antibody towards SARS-CoV-2. This latter is a pseudovirus prepared in artificial saliva that was used in this work. When the virus binds with the custom protein or antibody immobilized on the biosensor surface, the refractive index of the physical space occupied by the virus-antibody pair, which is also approximate to the biosensor surface, will increase, resulting in a redshift of the resonant-feature characteristics in the reflection spectrum of the biosensor. This resulting spectrum is measured twice before and after virus binding, and by calculating the amount of quantitative redshift information, the virus in the specimen can be obtained.

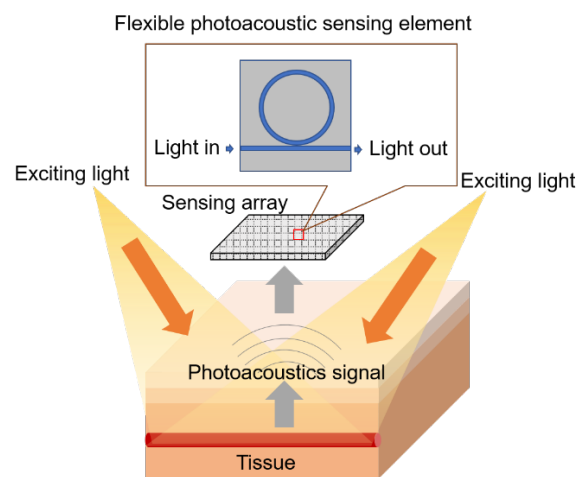


Fig. 3. Flexible electronic device for photoacoustic sensing.

### 2.2. Wearable photoacoustic imaging

Photoacoustic imaging (PAI) [7] is a non-invasive imaging technique without radiation, which combines the advantages of optical imaging and acoustic imaging. Based on the photoacoustic effect, a modulated pulse light can generate the ultrasound signals inside the tissue. And the photoacoustic signals can be received by the ultrasound transducers and reconstructed into images. Using endogenous light-absorbing contracts of biological tissues, PAI

can present the anatomical and functional information of different tissues, including hemoglobin, myoglobin, lipids, melanin, water, DNA, RNA, bilirubin, etc. [8], which can be used for disease detection and daily inspection.

Ultrasound sensor is one of the most important parts of a PAI system. Traditional ultrasound transducers detect the photoacoustic signal by converting pressure signals to electrical signals. The transducers have narrow bandwidth and are limited for further miniaturization [9]. The systems need transducer arrays or a scanner to increase the field of view, which restricts the size of the probe and the precision of the detection. Some researchers use integrated photonics to detect photoacoustic signals with sensors of great performance [9, 10]. Flexible devices will make transducers better in contact with human bodies, and they are one of the solutions for future wearable devices. Authors are integrating ultrasonic transducers on flexible substrates and use them for human body sensing [11, 12]. Figure 3 shows the schematic of flexible electronic systems intended for application in photoacoustic sensing.

### 2.3. Respiration monitoring and electrical/magnetic stimulation

Unfortunately patients with COVID-19 may be easy to be affected with upper airway obstruction [13]. This obstruction is a life-threatening disease which needs consistent assessment and either non-invasive or different invasive intervention methods [14]. Among series of methods to treat upper airway obstruction, electrical stimulation show potential high-performance solution [15]. The principle of electrical stimulation system to treat upper airway obstruction since the genioglossal muscle can be contracted when stimulating the hypoglossal nerve. The genioglossal muscle is the largest dilator muscle. With the contraction of this muscle, upper airway can be enlarged, and obstruction can be relieved and treated.

Figure 4 shows the breathing monitor and electrical stimulation system. This system consists of a respiratory detection unit and an electrical stimulation device. If patients are affected by upper airway obstruction, the respiratory waveform will be different from that of normal people. This respiratory difference can be detected through a pressure sensor. Recently, there are many detection methods of human breathing, which can be roughly divided into contact and non-contact respiratory monitoring techniques [16]. Compared to the non-contact respiratory method, contact approach possesses higher accuracy owing to direct contact with the body measurement. Among them, the flexible pressure sensor has the advantages of small size, and easy to be merged within clothing, which is selected to perform the respiratory monitoring task.

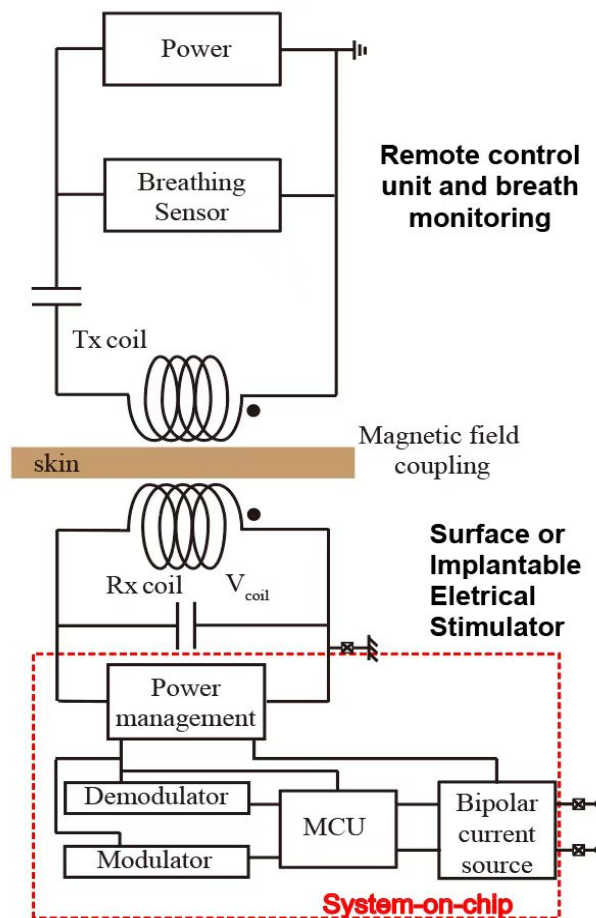


Fig. 4. Breathing monitor and subsequent electrical neurostimulation interface.

Previous studies have demonstrated the high sensitivity and conformality of our flexible pressure sensor, which lays the groundwork for subsequent respiratory detection [17]. Then, the respiratory monitoring unit transmits this abnormal respiratory signal to electrical stimulation block to apply stimulation process. Electrical stimulation block consists of power management module (rectifier, regulator), modulator, demodulator, control unit and bi-phasic current source.

Received electromagnetic voltage signal is converted to DC voltage level through power management module to supply power to the electrical stimulation module. The regulated DC voltage is used to initiate the stimulation process. The control unit of the electrical stimulation block updates the stimulating parameters to the stimulator's current source, which then applied to hypoglossal nerve after receiving the activation instruction from the respiratory monitoring circuit. Two alternative stimulation approaches are included: 1) Purely magnetic stimulation which is remotely applied from outside the body; 2) Electrical stimulation device to be implanted under the skin close by the hypoglossal nerve through two-contact electrodes for more critical cases.

### 3. Technical challenges and results

To achieve the goals of the proposed closed loop solution for fighting COVID-19, there are several technical issues that must be solved. The most important of them are representative of the major obstacles. Solving these issues will secure research breakthroughs of the proposed system.

### 3.1. Portable biosensing

Fully automatic, high-throughput, high-sensitivity and high-accuracy field detection of COVID-19. In view of the characteristics of COVID-19's rapid transmission and high risk of infection, the study of high-throughput detection method can achieve large-scale screening. The higher sensitivity can detect infected persons in early stage to isolate patients and apply early treatment. The fully automated system can avoid the infection of operators or the cross contamination between samples.

Expected coronavirus biosensors must be consumables, their design, and integration are intended for mass production potential. If they can be mass-produced, they can be deployed in a large area and play their potential in onsite detection. The mass production of biosensors also requires reliable and stable quality, which can maintain the validity of the biosensor to facilitate transportation and storage. The silicon wafer-level production of porous silicon has been industrialized, which has established a good foundation for the large-scale production of biosensors. Therefore, the proposed devices in this work are of great significance for preventing and controlling COVID-19 in a large-scale application.

Considering the nanopore selectivity and surface chemical characteristics of porous silicon biosensor, the requirements of sample pretreatment should be studied. For the whole detection process, the treatment of clinical samples is also of great significance for the detection results. Therefore, the development of pretreatment methods for different samples such as pharyngeal swab sampling, sputum or bronchoalveolar lavage fluid is very important to give full play to biosensor performance. Preliminary studies show universal viral medium (UVM) or universal transport medium (UTM) are good for saliva or swab collections, and the solution can be applied on biosensor surface directly with good specificity. More studies are needed to characterize effects of more complex samples, such as of patients with multiple infections and mixture from multiple patients.

Figure 5 shows representative spectral shifts of the biosensor upon binding reaction with N protein of SARS-CoV-2 (10 ng/ $\mu$ l). Biosensors loaded with N protein samples were measured every 1 min, as the N protein is captured by the antibody on the biosensor surface, the characteristic valley of the reflection spectrum shows a continuous red shift change.

### 3.2. Photoacoustic imaging

At present, X-ray CT is the familiar imaging technique for human lung detection [18], which is an important complement to NAAT and gene sequencing methods for COVID-19. However, CT is a radiation method, which is not safe for human to use frequently. And this technique can't be friendly used to neonate not only due to the radiation but also the instability of the detection, because neonates are active, who needs to be fixed by adults. Therefore, photoacoustic imaging (PAI) as a non-invasive imaging technique with high optical specificity and deep acoustic propagation depth, is expected to be used widely in COVID-19 related lung detection.

Ultrasonic sensors are the most important parts of the PAI systems. We focus on designing high-performance ultrasonic transducers, using integrated optical platform-based methods to detect photoacoustic signals. Based on the principle of the wearable photoacoustic imaging system, the structure of the photoacoustic probe is being designed. The pulsed light source is selected according to the property of the lung tissues. And the photoacoustic signal receiver will be made and combined with the sensor designed based on the integration method. Then the controller system, data acquisition, amplifier will be arranged considering the whole system structure and functions. And the algorithms for data processing and image reconstruction will be conducted.

Before designing the whole wearable photoacoustic imaging system, the interaction between the optical and acoustic

signals with lung tissues needs to be understood. Realizing the mechanism of the photoacoustic signal generation and propagation inside the lungs can prompt to acquire high-quality photoacoustic signals and images. Therefore, we conducted a simulation model of photoacoustic imaging for lung tissues using COMSOL Multiphysics software, to analyze the photoacoustic signal generation inside the lung tissues.

The method of our simulation was followed by the previous work [19]. Figure 6 shows the results of the simulation model of lung tissues with excitation of a pulsed light source. From the results, it can be known that the optical energy arrived at the object changes following with the change of the pulsed light.

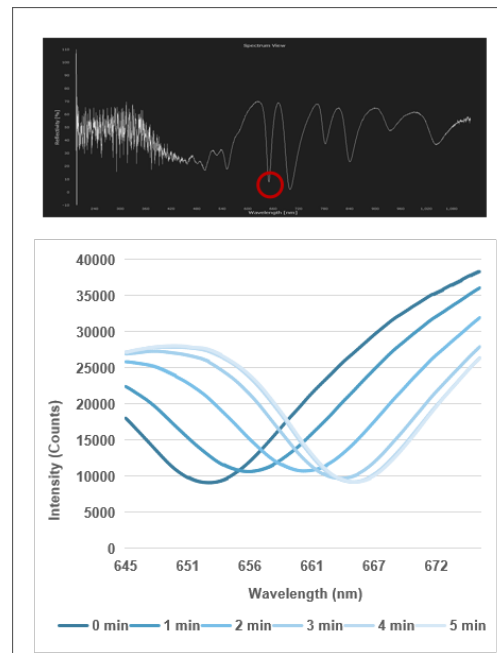


**Fig. 5.** Response of the biosensor for detection of SARS-CoV-2 N protein (10 ng/ $\mu$ l). Above: characteristic valley of the reflection spectrum used for tracking of spectral shift is circled by red. Below: real time shift of the characteristic valley as N protein of SARS-CoV-2 is binding with specific antibody.

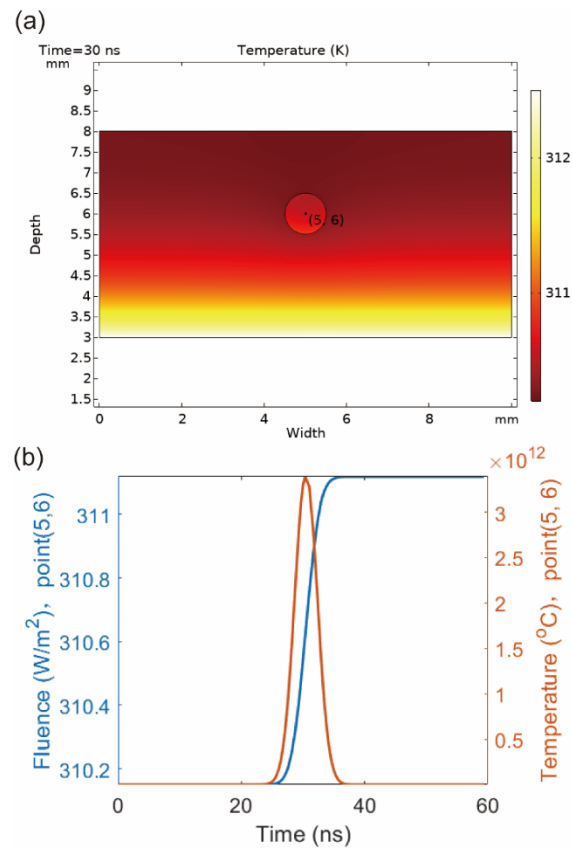


**Fig. 6.** Simulation results of photoacoustic imaging for lung tissues: (a) Temperature changes at 30 ns, (b) Optical fluence and temperature change from 0-60 ns at point (5, 6).

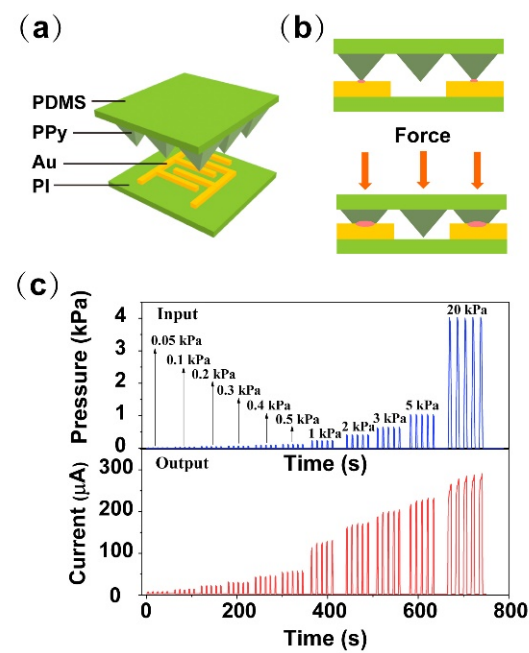


**Fig. 7.** Results of force sensor for respiration monitoring, (a-b) Working principle of the PPy based force sensor, (c) Current-time curves of the sensor with different applied forces.

The light energy reaches its maximum value when it is at the central time of one pulse at 30 ns. And the temperature increases accumulatively following the excitation, which can represent photoacoustic signal generation. Based on the simulation result, the potential of photoacoustic imaging for lung tissues is demonstrated.

### 3.3. Respiration monitoring and stimulation

Although currently some sensing techniques may already have high sensitivity for detecting respiratory rate, long-term device stability and wearing comfort are still challenging. Therefore, it is necessary to concentrate on the rapid development of devices with long-term stability, so that the accuracy of the device can be improved. In addition, searching for more appropriate materials to integrate breath sensors can improve wearing comfort while ensuring accuracy.

The electrical stimulation system includes a respiratory monitor unit and electrical stimulation unit. As shown in Figure 7(a), the respiratory monitor device is based on a micro-pyramidal resistive force sensor, which is composed of a polyimide (PI) substrate integrated with interdigitated Au electrodes and polydimethylsiloxane (PDMS) film with micro-pyramidal structure conformally coated with polypyrrole (PPy). The mechanism of the sensor is depicted in Figure 7(b), when the force is applied on the sensor, PPy-based micro-pyramidal film is deformed, which leads to increased contact area between interdigitated electrodes and PPy film, and therefore the resistance decreases. Figure 7(c) illustrates the instant current-time curve of respiration sensor under repeated loading/unloading of different force between 0.05 kPa to 20 kPa, which includes human respiration level.

On the other hand, electrical stimulation unit consists of two parts including communication and energy transfer through the inductive link. This link is built by two metal coils. One coil is placed outside the body. The other is embedded inside the body and under the skin. Generally, the power transfer efficiency of this inductive link is strongly related to the self-inductances of external coil  $L_1$  and internal coil  $L_2$ , mutual inductance  $M$ , load resistance, and the operating frequency  $f$ . Here, the operating frequency is confined to 13.56 MHz to meet the industrial, scientific, and medical radio band requirements.

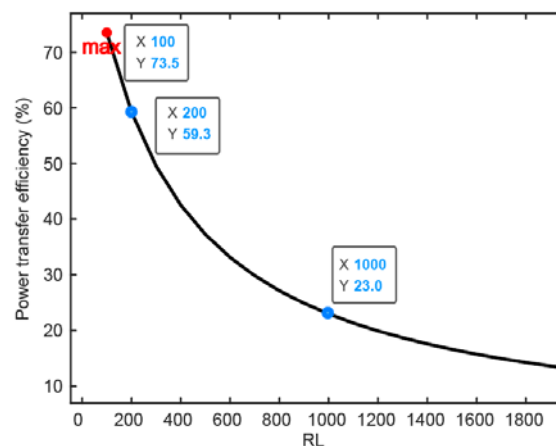


**Fig. 8.** COMSOL-based simulation results of magnetic field coupling link showing power transfer efficiency related to the load resistance.

Here, we have simulated the magnetic field of an inductive coupling link through COMSOL Multiphysics. The electrical stimulation target is the hypoglossal nerve, above which the tissue is slim. We mimic this tissue thickness as a gap of around 6 mm describing the distance between the external coil (Tx) and the internal coil (Rx). On the other hand, the diameter of the hypoglossal nerve is around 2.5 mm [20]. The internal coil would be placed upon this hypoglossal nerve, and its diameter is

designed as 1cm in consideration of needed power to be transferred for efficient stimulation of the hypoglossal nerve. The diameter of the Tx coil is defined as 5 cm.

The result of the simulation of power transfer efficiency of the inductive link is depicted in Figure 8 in function of the receiver overload. Through global evaluation, the self-inductances of the Tx and Rx are calculated as  $L_1 = 16.057 \mu\text{H}$ ,  $L_2 = 0.887 \mu\text{H}$ , respectively. The mutual inductance between these two coils is  $M = 0.441 \mu\text{H}$ . As we have illustrated above in Figure 4, the energy received by the internal coil would be input to the power management module (PMM), which means PMM works as a load connected to the inner coil. This load is named as RL in Figure 8. Based on the formula of PTE introduced in [21], PTE is strongly related to the value of RL. With process variation and transistor size, RL varies from  $100 \Omega$  to several k $\Omega$ . While the impedance between stimulation electrodes is around 1 k $\Omega$ , the maximum value of RL is analyzed as 2 k $\Omega$ . With the increase of RL, power transfer efficiency (PTE) decreases significantly. When RL is 1 k $\Omega$ , PTE can be 23%. In terms of power consumption, the load between two stimulation electrodes consumes 4 mW if the stimulation current is 2 mA. As system-on-chip (SOC) embedded in the body consumes around 10% of the load power budget, the whole power consumption of the implantable part is 4.4 mW. Combined with the simulation results of PTE of magnetic coupling link, the external power supply needs 22 mW at least.

## 4. Conclusion

The proposed closed-loop system includes several complementary topics, it consists of three subsystems. The wearable whole course surveillance, detection and stimulation system are suitable for fighting COVID-19 pneumonia or other kinds of infectious diseases. The implementation of the proposed system is intended to produce a series of achievements with clinical application value, which will be used in epidemic diagnosis, treatment, prevention, and control. Moreover, the scientific research results produced by the project can also be widely used in possible future epidemics requiring rapid, low-cost detection, prevention and control, and treatment measures. The system provides a range of fast, high-throughput, non-invasive, portable, or wearable solutions, to achieve rapid detection of infected patients, curbing the rapid spread of the current and future epidemics.

## Declarations of interest

None.

## Acknowledgement

This work was supported by the Leading Innovative and Entrepreneur Team Introduction Program of Zhejiang (grant number 2020R01005), Westlake University (grant number 10318A992001), Tencent Foundation (grant number XHTX202003001), Research Program on COVID-19 of Zhejiang University of Technology, and Zhejiang Key R&D Program (grant number 2021C03002).

## Abbreviations

COVID-19: coronavirus disease 2019; CT: computed tomography; DBR: distributed Bragg reflector; LSPR: localized surface plasmon resonance; NAAT: nucleic acid amplification test; PAI: photoacoustic imaging; PCR: polymerase chain reaction; SARS-CoV-2: severe acute respiratory syndrome coronavirus 2; UTM: universal transport medium; UVM: universal viral medium; CDC: Center for Disease Control.

## References

1. Jayamohan, H., Lambert, C.J., Sant, H.J., Jafek, A., Patel, D., Feng, H.D., Beeman, M., Mahmood, T., Nze, U. and Gale, B.K. SARS-CoV-2 pandemic: a review of molecular diagnostic tools including sample collection and commercial response with associated advantages and limitations. *Anal Bioanal Chem*, **2021**. 413(1): p. 49–71.
2. Larremore, D.B., Wilder, B., Lester, E., Shehata, S., Burke, J.M., Hay, J.A., Milind, T., Mina, M.J. and Parker, R. Test sensitivity is secondary to frequency and turnaround time for COVID-19 screening. *Sci Adv*, **2021**. 7(1): p. eabd5393.
3. Kim, S.-K., Koo, J., Lee, G.-H., Jeon, C., Mok, J.W., Mun, B.H., Lee, K.J., Kamrani, E., Joo, C.-K. and Shin, S. Wireless smart contact lens for diabetic diagnosis and therapy. *Sci Adv*, **2020**. 6(17): p. eaba3252.
4. Chi, W.X., Chen, Y., Wang, L.N., Luo, Z.Y., Zhang, Y. and Zhu, X.Y. Acupuncture for COVID-19 patient after ventilator weaning A protocol for systematic review and meta-analysis. *Medicine*, **2020**. 99(50).
5. Wu, C., Rong, G., Xu, J., Pan, S. and Zhu, Y. Physical analysis of the response properties of porous silicon microcavity biosensor. *Physica E: Low-Dimensional Systems & Nanostructures*, **2012**. 44(7–8): p. 1787–1791.
6. Rong, G., Y., Z., Li, X., Guo, M., Su, Y., Bian, S., Dang, B., Chen, Y., Zhang, Y., Yan, R.; et al. A high-throughput fully automatic biosensing platform for efficient COVID-19 detection. *Biosens. Bioelectron.*, **2022**. submitted.
7. Yang, X., Chen, Y.H., Xia, F. and Sawan, M. Photoacoustic imaging for monitoring of stroke diseases: A review. *Photoacoustics*, **2021**. 23: p. 100287.
8. Li, L. and Wang, L.V. Recent Advances in Photoacoustic Tomography. *BME Frontiers*, **2021**. p. 1-17.
9. Shnaiderman, R., Wissmeyer, G., Ulgen, O., Mustafa, Q., Chmyrov, A. and Ntziachristos, V. A submicrometre silicon-on-insulator resonator for ultrasound detection. *Nature*, **2020**. 585(7825): p. 372-378.
10. Westerveld, W.J., Mahmud-Ul-Hasan, M., Shnaiderman, R., Ntziachristos, V., Rottenberg, X., Severi, S. and Rochus, V. Sensitive, small, broadband and scalable optomechanical ultrasound sensor in silicon photonics. *Nature Photonics*, **2021**. 15(5): p. 341-345.
11. Jin, P., Fu, J., Wang, F., Zhang, Y., Wang, P., Liu, X., Jiao, Y., Li, H., Chen, Y., Ma, Y.; et al. A flexible, stretchable system for simultaneous acoustic energy transfer and communication. *Sci Adv*, **2021**. 7(40): p. eabg2507.
12. Hu, H., Zhu, X., Wang, C., Zhang, L., Li, X., Lee, S., Huang, Z., Chen, R., Chen, Z., Wang, C.; et al. Stretchable ultrasonic transducer arrays for three-dimensional imaging on complex surfaces. *Sci Adv*, **2018**. 4(3): p. eaar3979.
13. Min, S., Sorin, C. and Carino, G. Patient with recent COVID-19 infection presenting with acute upper airway obstruction. *Chest*, **2021**. 160(4): p. A375-A375.
14. Eskander, A., de Almeida, J.R. and Irish, J.C. Acute Upper Airway Obstruction. *New England Journal of Medicine*, **2019**. 381(20): p. 1940-1949.
15. Xia, F. and Sawan, M. Clinical and Research Solutions to Manage Obstructive Sleep Apnea: A Review. *Sensors*, **2021**. 21(5): p. 1784.

- 
16. Maurya, L., Kaur, P., Chawla, D. and Mahapatra, P. Non-contact breathing rate monitoring in newborns: A Review. *Computers in Biology and Medicine*, **2021**: p. 104321.
  17. Zhu, B., Ling, Y., Yap, L.W., Yang, M., Lin, F., Gong, S., Wang, Y., An, T., Zhao, Y. and Cheng, W. Hierarchically structured vertical gold nanowire array-based wearable pressure sensors for wireless health monitoring. *ACS Applied Materials & Interfaces*, **2019**. 11(32): p. 29014-29021.
  18. Shirani, F., Shayganfar, A. and Hajiahmadi, S. COVID-19 pneumonia: a pictorial review of CT findings and differential diagnosis. *Egyptian Journal of Radiology and Nuclear Medicine*, **2021**. 52(1).
  19. Yang, X., Chen, Y.H. and Sawan, M. Photoacoustic Generation in Human Brain with Embedded Blood Vessel: Modeling and Simulation. in *2021 Photonics & Electromagnetics Research Symposium (PIERS)*. **2021**.
  20. Xia, F., and Sawan, M., "Electrode-Nerve Interface Properties to Treat Patients with OSA through Electrical Stimulation," *2021 Sixth International Conference on Advances in Biomedical Engineering (ICABME)*, **2021**, pp. 121-124.
  21. Ibrahim, A., and Kiani, M., "A figure-of-merit for design and optimization of inductive power transmission links for millimeter-sized biomedical implants," *IEEE Transactions on Biomedical Circuits and Systems*, vol. 10, no. 6, **2016**, pp. 1100–1111.